Nitric Oxide 83 (2019) 40–50

Contents lists available at ScienceDirect

Nitric Oxide

journal homepage: www.elsevier.com/locate/yniox

Age- and sex-related changes in cortical and striatal nitric oxide synthase in the Q175 mouse model of Huntington's disease

Fernando E. Padovan-Neto[a,*,1], Lauren Jurkowski[a], Conor Murray[a], Grace E. Stutzmann[a], Mei Kwan[b], Afshin Ghavami[b], Vahri Beaumont[c], Larry C. Park[c], Anthony R. West[a]

[a] Department of Neuroscience, The Chicago Medical School at Rosalind Franklin University of Medicine and Science, North Chicago, IL, USA
[b] PsychoGenics Inc., Paramus, NJ, USA
[c] CHDI Management/CHDI Foundation, Los Angeles, CA, USA

ARTICLE INFO

Keywords:
Huntington's disease
NADPH-Diaphorase
Nitric oxide synthase
Striatum
Cortex

ABSTRACT

In Huntington's disease (HD), corticostriatal and striatopallidal projection neurons preferentially degenerate as a result of mutant huntingtin expression. Pathological deficits in nitric oxide (NO) signaling have also been reported in corticostriatal circuits in HD, however, the impact of age and sex on nitrergic transmission is not well characterized. Thus, we utilized NADPH-diaphorase (NADPH-d) histochemistry and qPCR assays to assess neuronal NO synthase (nNOS) activity/expression in aged male and female Q175 heterozygous mice. Compared to age-matched controls, male Q175 mice exhibited reductions in NADPH-d staining in the motor cortex at 21, but not, 16 months of age. Comparisons across genotypes showed that striatal NADPH-d staining was significantly decreased at both 16 and 21 months of age. Comparisons within sexes in 21 month old mice revealed a decrease in striatal NADPH-d staining in males, but no changes were detected in females. Significant correlations between cortical and striatal NADPH-d staining deficits were also observed in males and females at both ages. To directly assess the role of constitutively active NOS isoforms in these changes, nNOS and endothelial NOS (eNOS) mRNA expression levels were examined in R6/2 (3 month old) and Q175 (11.5 month old) mice using qPCR assays. nNOS transcript expression was decreased in the cortex (40%) and striatum (54%) in R6/2 mice. nNOS mRNA down-regulation in striatum of Q175 animals was more modest (19%), and no changes were detected in cortex. eNOS expression was not changed in the cortex or striatum of Q175 mice. The current findings point to age-dependent deficits in nNOS activity in the HD cortex and striatum which appear first in the striatum and are more pronounced in males. Together, these observations and previous studies indicate that decreases in nitrergic transmission progress with age and are likely to contribute to corticostriatal circuit pathophysiology particularly in male patients with HD.

1. Introduction

Huntington's disease (HD) is an autosomal dominant neurodegenerative disorder caused by abnormal expansion in CAG trinucleotide repeats within the *huntingtin* gene encoding for the huntingtin protein [1]. In HD, medium-sized spiny neurons (MSNs) projecting to the external globus pallidus (i.e., indirect pathway) are thought to preferentially degenerate as a result of accumulation of the mutant huntingtin protein and the formation of polyglutamine-containing inclusion bodies [2–4]. Striatal parvalbumin expressing GABAergic interneurons (fast-spiking interneurons) are also lost in HD [5]. Conversely, striatal interneurons expressing choline acetyltransferase (cholinergic interneurons) and NADPH-diaphorase (NADPH-d) activity/neuropeptide Y/somatostatin (neuronal nitric oxide synthase expressing interneurons; nNOS) are spared [6–9], potentially because these interneurons do not express the NR2B subunits of the NMDA receptor [10]. Additional evidence points to widespread volume decreases in the cerebral cortex and related structures [11,12] and degeneration of corticostriatal projection neurons (reviewed in Refs. [13,14].

Dysregulation of glutamate and dopamine transmission [13,15] and deficits in striatal nitric oxide (NO) synthesis and cyclic nucleotide production/metabolism have also been reported in HD and animal

* Corresponding author. Department of Psychology, Faculty of Philosophy, Sciences and Letters of Ribeirão Preto, University of São Paulo, Av. Bandeirantes 3900, 14040-901, São Paulo, SP, Brazil.
E-mail address: ferpadovan@usp.br (F.E. Padovan-Neto).
[1] Current address: Department of Psychology, Faculty of Philosophy, Sciences and Letters of Ribeirão Preto, University of São Paulo, São Paulo, SP, Brazil.

https://doi.org/10.1016/j.niox.2018.12.002
Received 25 April 2018; Received in revised form 19 November 2018; Accepted 3 December 2018
Available online 05 December 2018
1089-8603/ © 2018 Elsevier Inc. All rights reserved.

models [16–19], effects which may be linked to neuroanatomical abnormalities in cortical and striatal excitatory synapses [20] and aberrant corticostriatal transmission [21,22]. Interestingly, we have shown that cortical stimulation increases striatal NO synthase (NOS) activity via an NMDA and dopamine D1 receptor dependent mechanism [23–26]. Activation of striatal interneurons expressing neuronal NOS (nNOS) acts to amplify glutamateric corticostriatal transmission, increase synaptic plasticity, and drive MSN output in intact rats (Reviewed in Refs. [27,28]. Furthermore, our recent studies in nNOS knockout mice demonstrating that striatal MSNs are substantially less responsive to cortical drive as compared to wild-type (WT) controls, indicate that NO signaling is critically involved in maintaining corticostriatal transmission [29]. Thus, deficits in nNOS activity and NO signaling observed in HD could be associated with decreased excitatory corticostriatal transmission and motor dysfunction. This is supported by studies showing that nNOS mRNA and NADPH-d staining is reduced in the striatum of HD patients in a manner that becomes more pronounced with disease progression [19,30]. Furthermore, laser-microdissection studies of striatal nNOS interneurons in HD mice found that nNOS mRNA levels are reduced by ~40% compared to WT mice [10]. Other studies have revealed that nNOS protein expression and activity are decreased in the motor cortex and/or striatum of R6/1 and R6/2 mice in a manner that is associated with body weight loss and motor activity deficits [31–35].

Taken together, the above studies indicate that deficits in cortical and striatal nNOS activity and nitrergic transmission may contribute to the progression of corticostriatal pathway dysfunction observed in HD. To begin to examine age- and sex dependent changes in nNOS activity in HD, the current study utilized the Q175 knock in mouse model which incorporates a CAG trinucleotide expansion of the human mutant *huntingtin* gene (mHtt) to accurately reproduce the full behavioral HD phenotype [36–38]. Histochemical assessment of NADPH-d staining was employed to assess nNOS activity in striatum and motor cortex (M1 area) in aged male and female Q175 heterozygous mice (16 and 21 months of age). Lastly, qPCR was utilized to determine whether changes observed in histochemical studies are related to dysregulation of mRNAs encoding constitutively active NOS isoforms (nNOS and endothelial NOS (eNOS)) in R6/2 (3 month old) and Q175 (11.5 month old) mice.

2. Materials and methods

2.1. Chemicals

Reduced NADPH and formalin were purchased from Sigma (St. Louis, MO). Nitroblue tetrazolium was purchased from Tocris (Ellisville, MO). In qPCR studies, a Universal Probe Library was purchased from Roche Applied Science (Indianapolis, IN). Gene specific primers were purchased from Sigma (St. Louis, MO). All other reagents were of the highest grade commercially available.

2.2. Subjects

WT and heterozygous (HET) z_Q175 transgenic mice (Q175 mice) expressing the human mHtt allele with the expanded CAG repeat within the native mouse *huntingtin* gene, and R6/2_transgenic mice (R6/2–120 CAG repeats, Table 1) were obtained from the Jackson Laboratory (Bar Harbor, Maine) or, in the case of qPCR studies, from in house breeding colonies at PsychoGenics, Inc. (Tarrytown, NY). All NADPH-d histochemistry studies were performed at Rosalind Franklin University of Medicine and Science. All qPCR studies were performed at PsychoGenics, Inc. Mice were housed five per cage under conditions of constant temperature (21–23 °C) and maintained on a 12:12-h light/dark cycle with food and water available ad libitum. All animal procedures were approved by the Rosalind Franklin University of Medicine and Science or PsychoGenics Inc., Institutional Animal Care and Use Committees and adhere to the Guide for the Care and Use of Laboratory Animals published by the United States Public Health Service.

2.3. Histology

Brains were extracted and immersed in a 30% sucrose/10% formalin solution for 24 h, then frozen over dry ice and stored at −80 °C. Brains were cut on a cryostat to obtain 40-μm-thick coronal sections and were stored at −20 °C in cryoprotectant solution until all groups were processed (~4 weeks). In order to produce accurate and non-biased sampling of cortical and striatal subregions, four standardized coronal sections were selected from each mouse brain (Fig. 1, top), which corresponded to stereotaxic coordinates representative of the rostral and medial striatum (+1.09, +0.73, +0.37 and + 0.13 anterior to bregma as determined using the atlas of Paxinos and Franklin [39].

2.4. NADPH-d histochemistry

NADPH-d staining was performed with minor modifications as described previously [23,40]. In order to reduce variation in stain intensity and maximize the signal to noise ratio of the NADPH-d reaction, brains from all treatment groups were processed together an identical manner using the same solutions to minimize group differences in histochemical reactions. Free-floating sections were washed three times (5 min) in 0.1 M phosphate-buffered (PB) solution, washed once (20 min) in 0.05 M PB solution containing 0.6% Triton X-100, and incubated at 37 °C for (60 min) in 0.025 M PB solution containing 0.3% Triton X-100, 0.1 mg/mL nitroblue tetrazolium and 1.0 mg/ml β-NADPH. Sections were then allowed to cool down to room temperature (10 min) and were washed three times (5 min each) in 0.1 M PB solution. Sections were then mounted on gelatinized slides, dehydrated, and cover slipped.

2.5. Total RNA extraction

Cortical and striatal tissues were homogenized 2 × 1 min at 25 Hz in 750 μL of QIAzol Lysis Reagent (Cat # 79306, Qiagen, Valencia, CA) with TissueLyser (Qiagen, Valencia, CA) and 5 mm stainless steel beads (Cat # 69989, Qiagen, Valencia, CA). Once tissues were disrupted, samples were allowed to incubate at room temperate for 5 min. For RNA extraction, manufacturer protocol for RNeasy 96 Universal Tissue Kit (Cat # 74881, Qiagen, Valencia, CA) for RNA isolation was followed. Briefly, 150 μL of Chloroform (Cat #C2432, Sigma-Aldrich, St.

Table 1
CAG repeat length across age groups and sex in NADPH-diaphorase and nNOS/eNOS transcript studies.

	3 months	11.5 months	16 months	21 months
Male Q175		188.5 ± 2.07 (6)	189.5 ± 2.9 (6)	189.3 ± 2.1 (8)
Female Q175		187.4 ± 2.52 (5)	184.3 ± 1.3 (9)	193.5 ± 1.5 (6)
Male R62	121.6 ± 1.96 (7)			
Female R62	120.2 ± 1.46 (7)			

$p > 0.05$. Data are presented as the mean ± SEM. The N of each group is in parentheses.

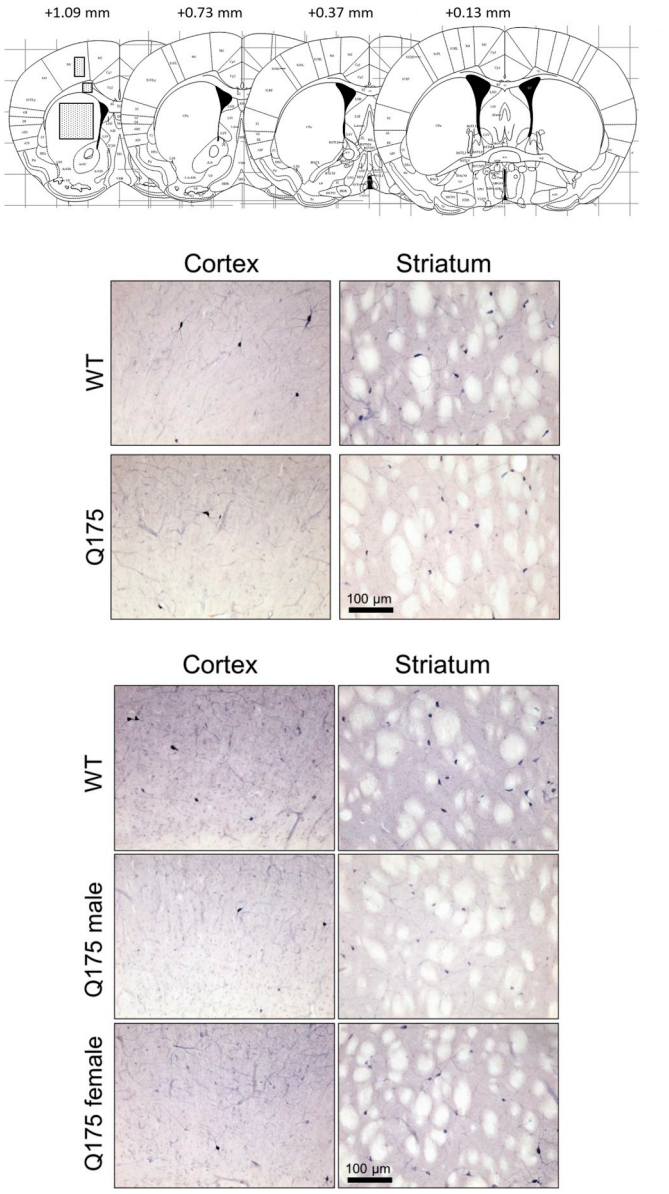

Fig. 1. Quantification of genotype-, age-, and sex-induced changes in NADPH-d staining in subregions of the motor cortex and striatum. Top) Diagrams showing the regions of interest (boxes) for quantification of NADPH-d staining in the mouse striatum and cortex (atlas of Paxinos and Franklin [39]. For both cortex and striatum, the gray levels of the region of interest in the right and left hemispheres of each of the four representative coronal sections were measured. The corpus callosum was used as a comparison area for the generation of measures of nonspecific staining. Gray level values measured in the corpus callosum were subtracted from those measured in the striatum or motor cortex to give a relative optical density value. **Middle)** Representative images of NADPH-d staining observed in the cortex and striatum of WT (top) and Q175 mice (bottom). **Bottom)** Representative images of NADPH-d staining observed in the cortex (left) and striatum (right) of WT (top), male Q175 (middle) and female Q175 mice (bottom). All images were taken at 20X magnification.

Louis, MO) was added and samples were shaken vigorously for 15 s followed by a 3-min incubation at room temperature. The aqueous phase was separated from the organic phase by centrifugation at 6000 × *g* (Beckman Coulter Avanti J-30I), 4 °C for 15 min. The aqueous phase was transferred to a new 96-well block and total RNA was precipitated with equal volume of 70% ethanol. RNA mixture was transferred to an RNeasy 96-well plate followed by centrifuge at 6000 × *g* (Beckman Coulter Avanti J-30I), at room temperate for 4 min. Total RNA bound to column membranes was treated with RNase-Free DNase set (Cat # 79254, Qiagen, Valencia, CA) for 30 min, followed by 3 washing steps with RW1 and RPE buffers (provided with RNeasy 96 Universal Tissue Kit). RNA was eluted with 40 µL RNase-Free water.

2.6. Total RNA quantification and reverse transcription

Working stocks of RNA was prepared at 10 ng/µl (for 0.1 µg RNA reverse transcription) with RNase-free water. RNA concentrations of the stock and working stock RNA samples were measured by OD260 and OD280 readings using the Nanodrop 8000 (Thermo Scientific). Five hundred nanogram of total RNA was reverse transcribed into cDNA with 3.2 µg random hexamers (Cat # 11034731001, Roche Applied Science, Indianapolis, IN), 1 mM each dNTP (Cat # 11814362001), Roche Applied Science, Indianapolis, IN), 20U Protector RNase Inhibitor (Cat # 03335402001, Roche Applied Science, Indianapolis, IN), 1X Transcriptor Reverse Transcription reaction buffer, and 10U Transcriptor Reverse Transcriptase (Cat # 03531287001, Roche Applied Science, Indianapolis, IN) in 20 µL total volume. Only 1 RT was prepared from each RNA sample and each RT sample was assayed by qPCR in triplicates. Note that reverse transcription reactions were assembled on CoolSafe PCR Tube Cooling Chambers (Diversified Biotech) to ensure all reaction components were at 4 °C prior to initiation of RT. The reactions were allowed to proceed at room temperature for 10 min, followed by 55 °C for 30 min, and then inactivated at 85 °C for 5 min in Gene Amp PCR Systems 9700 thermal cycler (Applied Biosystems, Foster City, CA). cDNA samples were diluted 10 fold with RNase-Free water for qPCR analysis.

2.7. Quantitative PCR (qPCR)

For all the assays in this study, the ABI Fast Block was used; 5 µl of the diluted cDNA was amplified with 20 µl 2X ABI Fast Start Master Mix, 0.2 µl Universal Probe Library Probe (Roche), 200 nM of each gene specific primer (Sigma, HPLC purified) in 20 µl reaction volume. Conditions for Fast Block qPCR were 95 °C for 20 s for activation of Taq DNA Polymerase followed by 40 cycles of 95 °C for 1 s and 60 °C for 20 s. For primers and probesused for qPCR please refer to Table 2.

cDNA prepared z_Q175KI Het or R62 whole brain RNA was used as calibrator (calibrator is diluted same as sample cDNA) for each of the respective HD model, to normalized plate to plate variations. See Table 2 for PCR efficiencies of the qPCR assays in this study. Each cDNA sample (diluted 1:10) from each RT was assayed in triplicates and the Ct values averaged. Values which lie greater than 0.25 standard deviation of the average were discarded. Relative quantity of the PCR product (relative to the calibrator) was calculated as follows:

$$\text{Relative Quantity of Target gene} = (\text{PCR Efficiency Target})^{(\text{Ct calibrator} - \text{Ct sample})}$$

$$\text{Relative Quantity of Housekeeping Gene 1} = (\text{PCR Efficiency housekeeping1})^{(\text{Ct calibrator} - \text{Ct sample})}$$

$$\text{Relative Quantity of Housekeeping Gene 2} = (\text{PCR Efficiency housekeeping2})^{(\text{Ct calibrator} - \text{Ct sample})}$$

$$\text{Relative Quantity of Housekeeping Gene 3} = (\text{PCR Efficiency housekeeping3})^{(\text{Ct calibrator} - \text{Ct sample})}$$

Geometric mean for the three housekeeping genes was calculated as follows:

$$\text{Geometric mean} = (\text{relative quantity of housekeeping gene 1} * \text{relative quantity of housekeeping gene 2} * \text{relative quantity of housekeeping gene 3})^{(1/3)}$$

Relative level of target gene was calculated as follows:

$$\text{Relative Quantity of Target gene} / \text{Geometric mean of housekeeping}$$

Table 2
qPCR primers and probe information.

Mouse Gene ID	5′ Primer Sequence	3′ Primer Sequence	Universal Probe Library #	Hydrolysis Probe (6-FAM)	Tissue	PCR Efficiency	R^2 Value of Std Curve
nNOS	GGCCACCAATGAGAAAGAGA	TATTCCTGAAGCCCCTTGC	66	N/A	Cortex Striatum	1.87	0.9976
eNOS	ATCCAGTGCCCTGCTTCA	GCAGGGCAAGTTAGGATCAG	12	N/A	Cortex Striatum	1.86	0.9953
ATP5B	GGCACAATGCAGGAAAGG	TCAGCAGGCACATAGATAGCC	77	N/A	Striatum Cortex	1.93	0.9995
CANX	TTCCAGACCCTGATGCAGA	TCCCATTCTCGGTCCATATC	106	N/A	Cortex	2.05	0.9944
RPL13A	TTGTGGCCAAGCAGGTACT	GTTGATGCCTTCACAGCGTA	77	N/A	Cortex	2.05	0.9934
Eif4A2	GCCAGGGACTTCACAGTTTC	TTCCCTCATGATGACATCTCTTT	93	N/A	Striatum	1.92	0.9932
GAPDH	CAATGTGTCCGTCGTGGATCT	GTCCTCAGTGTAGCCCAAGATG	N/A	CGTGCCGCCTGGAGAAACCTGCC	Striatum	1.89	0.9972

genes

Relative level of target gene was then normalized to tissue- and age-matched wild type cohorts.

2.8. Data analysis of NADPH-d histochemistry

Slides were visualized at 2X using light microscopy (Olympus BX60, Olympus, USA) and images were digitized using a Nikon DM1200 camera and ACT software (Nikon Microscopy, USA). All photographs were taken under constant controlled light conditions and optimized to avoid signal saturation. All camera, microscope and light settings were kept constant until the end of the analysis. The gray levels [41] of areas containing nNOS cell bodies, dendrites, and axons were measured using the Image J software (version 1:43; http://www.rsbweb.nih.gov/ij/, NIH) as described previously [23,40] and indicated in Fig. 1. All images were calibrated and pixels were converted to mm. The sampled striatal area consisted of a box measuring 1.2 by 1.2 mm and the sampled motor cortex (M1) area consisted of a box measuring 0.2 by 0.4 mm. A sample area was also taken from the corpus callosum (0.2 by 0.2 mm). Gray levels of the selected regions were measured on a scale ranging from 0 to 255 (0 representing the darkest labeling). Average cortical and striatal gray level values were measured and average background staining in the white matter of the corpus callosum was subtracted from these values. Measures were obtained from each subregion (i.e., striatum and cortex) within both the right and left hemispheres of all four coronal sections. We first compared right and left sides on each one of the four coronal sections and we found no difference of gray levels between hemispheres ($p > 0.05$, *t*-test). We then averaged data obtained from right and left hemispheres and compared gray levels across all four coronal sections for each subregion. Since we found no difference between gray levels measured across the four coronal sections ($p > 0.05$, one-way ANOVA), data was averaged to give a value for each subregion (Fig. 1). In addition, slides from each treatment group were tested for uniform light transmission through the blank portions of the slide to ensure consistency within measures across groups.

2.9. Statistical analysis

Genotype- and sex-induced changes in measures of NADPH-d staining was determined at 16 and 21 months of age using a two-way ANOVA with a Bonferroni post-hoc multiple comparison test. To analyze if NADHP-d staining changes occur uniformly in both cortex and striatum, Pearson correlations were conducted in male and female mice. Quantitative PCR data were analyzed by unpaired *t*-test. Values which fell above or below 2 standard deviations from the mean were considered statistical outliers and removed from the analysis. The statistical power of animal group sizes were determined using a power analysis. All measurements are expressed as mean ± SEM and the differences between experimental conditions were considered statistically significant when $p < 0.05$.

3. Results

Data from histochemical experiments are derived from 31 WT to 29 HET Q175 mice. Data from qPCR experiments are derived from 24 WT, 14 R6/2, and 11 HET Q175 mice. All Q175 mice were genotyped prior to experimentation and were found to have a range of 176–197 CAG repeats (mean = 188.7 ± 1.1). No significant differences in CAG repeat length were observed across age groups or sex ($p > 0.05$, *t*-test; Table 1). Initial comparisons across genotypes of all mice (both genders and age groups) revealed that both cortical and striatal NADPH-d staining was significantly reduced in 16–21 month old mice (unpaired *t*-test, $p < 0.01$; Fig. 2A and B). Examples of representative NADPH-d staining in the cortex and striatum of WT and Q175 mice are shown in Fig. 1 (middle).

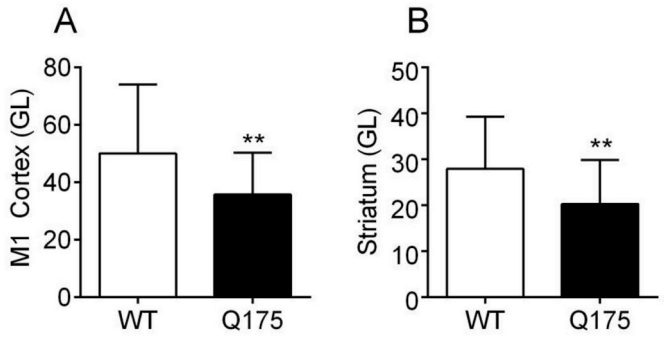

Fig. 2. Between groups comparison of effects of genotype on NADPH-d staining in motor cortex and striatum of all WT and Q175 mice 16–21 months of age. A) The mean ± S.E.M. NADPH-d staining in M1 motor cortex was reduced in Q175 het mice compared with WT controls (unpaired *t*-test, **p > 0.01). **B)** The mean ± S.E.M. NADPH-d staining in the striatum was reduced in Q175 het mice compared with WT controls (unpaired *t*-test, **p < 0.01). Data are derived from n = 31 WT and n = 29 Q175 mice.

Effects of genotype and sex on NADPH-d staining in the motor cortex and striatum: studies in 16 month old male and female WT and Q175 mice.

Further comparisons across genotypes within 16 month old male and female mouse groups indicated that no significant changes in NADPH-d staining occurred in the motor cortex of male or female mice as compared to age-matched WT controls (Fig. 3A, two-way ANOVA, $p > 0.05$). An overall effect of genotype on NADPH-d staining was observed in the dorsal striatum of 16 month old male and female mice (Fig. 3B, two-way ANOVA, $p < 0.05$), however pair-wise comparison's were not significant (Bonferroni's post-hoc test, $p > 0.05$). A significant correlation between NADPH-d staining levels in the motor cortex and striatum was observed in both male (Fig. 3C) and female (Fig. 3D) WT/Q175 mice, indicating that changes in NADPH-d activity in corticostriatal circuits may be interrelated (Pearson, $p < 0.0001$ (male), $p < 0.001$ (female)). Examples of representative NADPH-d staining in the cortex and striatum of WT and male/female Q175 mice are shown in Fig. 1 (bottom).

Effects of genotype and sex on NADPH-d staining in the motor cortex and striatum: studies in 21 month old male and female WT and Q175 mice.

An overall effect of genotype on NADPH-d staining was observed in both the motor cortex (Fig. 4A) and dorsal striatum (Fig. 4B) of 21 month old male and female mice (two-way ANOVA, $p < 0.01$ and $p < 0.05$, respectively). Additionally, pair-wise comparison's revealed that cortical NADPH-d staining was significantly reduced in 21 month old male (Bonferroni's post-hoc test, $p < 0.01$), but not female ($p > 0.05$), mice (Fig. 4A). Pair-wise comparisons within sexes in 21 month old mice also revealed a decrease in striatal NADPH-d staining in males compared to WT controls (Fig. 4B, Bonferroni's post-hoc test, $p < 0.05$), but no changes were detected in females ($p > 0.05$) as compared to age-matched WT controls. A significant correlation between NADPH-d staining levels in the motor cortex and striatum was observed in 21 month old male (Fig. 4C) and female (Fig. 4D) WT/Q175 mice, however these changes were more highly correlated in males compared to females (Pearson, $p < 0.0001$ (male), $p < 0.05$ (female)).

Effects of genotype on nNOS and eNOS mRNA expression in the

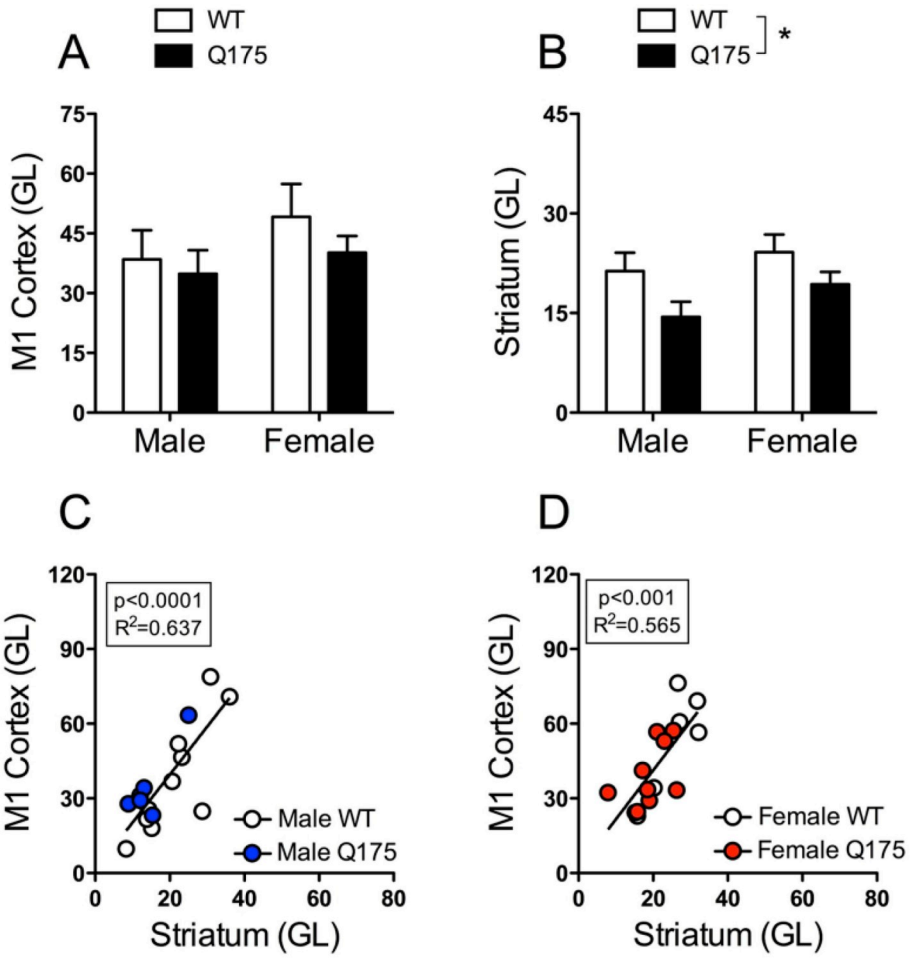

Fig. 3. Between groups comparison of effects of genotype and sex on NADPH-d staining in motor cortex and striatum of WT and Q175 mice at 16 months of age. A) The mean ± S.E.M. NADPH-d staining in M1 motor cortex was similar between 16 month old WT and Q175 het mice groups (two-way ANOVA, $p > 0.05$). **B)** The mean ± S.E.M. NADPH-d staining in the striatum was reduced in 16 month old Q175 het mice compared with age-matched WT controls (two-way ANOVA, *p < 0.05). Correlations between NADPH-d staining levels in M1 motor cortex and striatum of **C)** male and **D)** female mice revealed that NADHP-d staining changes uniformly in both structures (Pearson, $p < 0.0001$ (male), $p < 0.001$ (female)). Data are derived from 17 WT mice (n = 10 male, n = 7 female) and 15 Q175 mice (n = 6 male, n = 9 female).

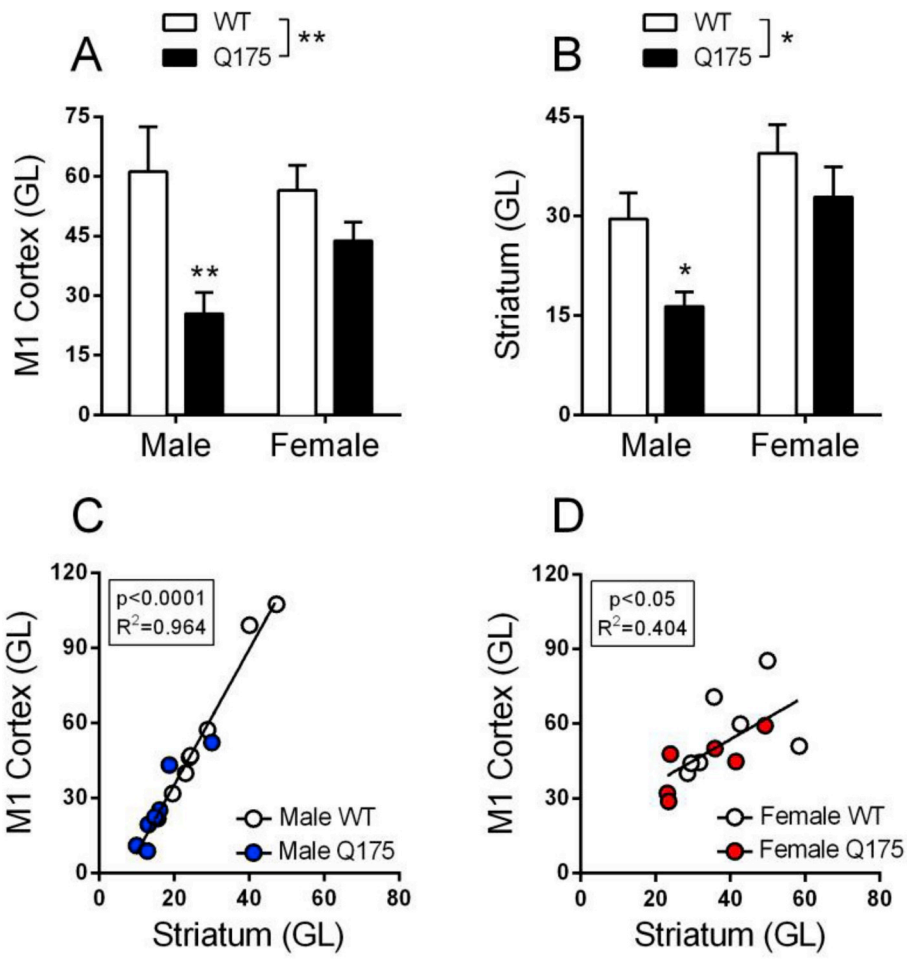

Fig. 4. Between groups comparison of effects of genotype and sex on NADPH-d staining in motor cortex and striatum of WT and Q175 mice at 21 months of age. A) The mean ± S.E.M. NADPH-d staining in M1 motor cortex was reduced in 21 month old Q175 het mice (two-way ANOVA, **p < 0.01). Bonferroni's post-hoc multiple comparison test revealed a significant reduction in cortical NADPH-d staining in male Q175 het mice compared with age-matched male WT controls (**p < 0.01). NADPH-d expression was reduced 58.42% in males and 22.46% in females compared with the respective WT controls. **B)** The mean ± S.E.M. NADPH-d staining in the striatum was reduced in Q175 het mice compared with WT controls (two-way ANOVA, *p < 0.05). Bonferroni's post-hoc multiple comparison test revealed a decrease in NADPH-d staining in male Q175 het mice compared with age-matched male WT controls (*p < 0.05). NADPH-d expression was reduced 44.67% in males and 16.77% in females compared with the respective WT controls. Correlations between NADPH-d levels in M1 motor cortex and striatum of **C)** male and **D)** female mice revealed that NADHP-d staining changes uniformly in both structures (Pearson, p < 0.0001 (male), p < 0.05 (female)). Data are derived from 14 WT mice (n = 7 male, n = 7 female) and 14 Q175 mice (n = 8 male, n = 6 female).

motor cortex and striatum: studies in male and female WT, R6/2 and Q175 mice.

To directly assess the potential role of constitutively active NOS isoforms in changes observed with histochemical measures, nNOS and eNOS mRNA expression levels were examined in male and female WT and Q175 (HET, 11.5 month old) mice using qPCR assays. Parallel studies were performed in WT and R6/2 mice (3 month old) in order to compare potential changes in Q175 mice to outcomes from a well characterized model of HD. A younger age group of Q175 mice (i.e., 11.5 versus 16–21 months of age) was used to determine if potential changes in NOS expression also occur first in striatum versus motor cortex as observed in histochemical studies. No differences in nNOS or eNOS transcript expression were observed across sexes in HD models at these ages ($p > 0.05$, data not shown), thus male and female mice were combined for the overall analysis of genotype effects. As shown in Fig. 5A, nNOS transcript expression was decreased in the cortex and striatum of 3 month old R6/2 animals (40% and 54% respectively, unpaired *t*-test, $p < 0.0001$). nNOS mRNA was also down-regulated in striatum of Q175 mice (Fig. 5B), although this decrease was more modest (19%, unpaired *t*-test, $p < 0.01$) than changes observed in the R6/2 striatum (Fig. 5A). No significant effects of the Q175 genotype were observed in the cortex in 11.5 month old mice ($p > 0.05$).

Expression of eNOS mRNA was also decreased in striatum of 3 month old R6/2 mice (Fig. 6A, 18%, unpaired *t*-test, $p < 0.01$). No significant effects of genotype were observed in the cortex (Fig. 6A, $p > 0.05$). Furthermore, eNOS transcript levels were unaffected in both the striatum and cortex of 11.5 month old Q175 mice (Fig. 6B, $p > 0.05$).

4. Discussion

To our knowledge, the current study is the first to examine potential effects of age and sex on changes in cortical and striatal nNOS activity and expression in WT and heterozygous Q175 mice. Consistent with studies in the R6/1 and R6/2 mouse models of HD [10,31,33,35], we observed significant deficits in striatal NADPH-d activity measured in Q175 mice at 16 and 21 months of age. Q175 mice also exhibited significant reductions in NADPH-d staining in the motor cortex at 21, but not, 16 months of age. Additionally, nNOS mRNA was down-regulated in a striatal-specific manner as early as 11.5 months of age in Q175 mice. nNOS transcript expression was also substantially decreased in the cortex and striatum of 3 month old R6/2 mice. Together these observations indicate that deficits in nNOS activity in motor cortex and striatum are likely to occur in mice expressing the full HD phenotype, and that striatal changes precede effects of mHtt on NO synthesis in the cortex. Furthermore, age-matched male Q175 mice, but not females, exhibited more robust decreases in cortical and striatal NADPH-d staining at 21 months of age. Significant correlations in cortical and striatal NADPH-d activity were also observed in male and female Q175 mice at both ages, suggesting that deficits in nitrergic transmission in both structures may be interrelated in HD. Taken together, these observations indicate that deficits in nNOS activation are present in corticostriatal systems in late stages of HD and are more severe in aged male animals.

4.1. Deficits in neuronal NOS activity in the Q175 mouse model of HD

It has been demonstrated that the catalytic domain of the NOS enzyme is responsible for NADPH-d activity, conversion of the substrate

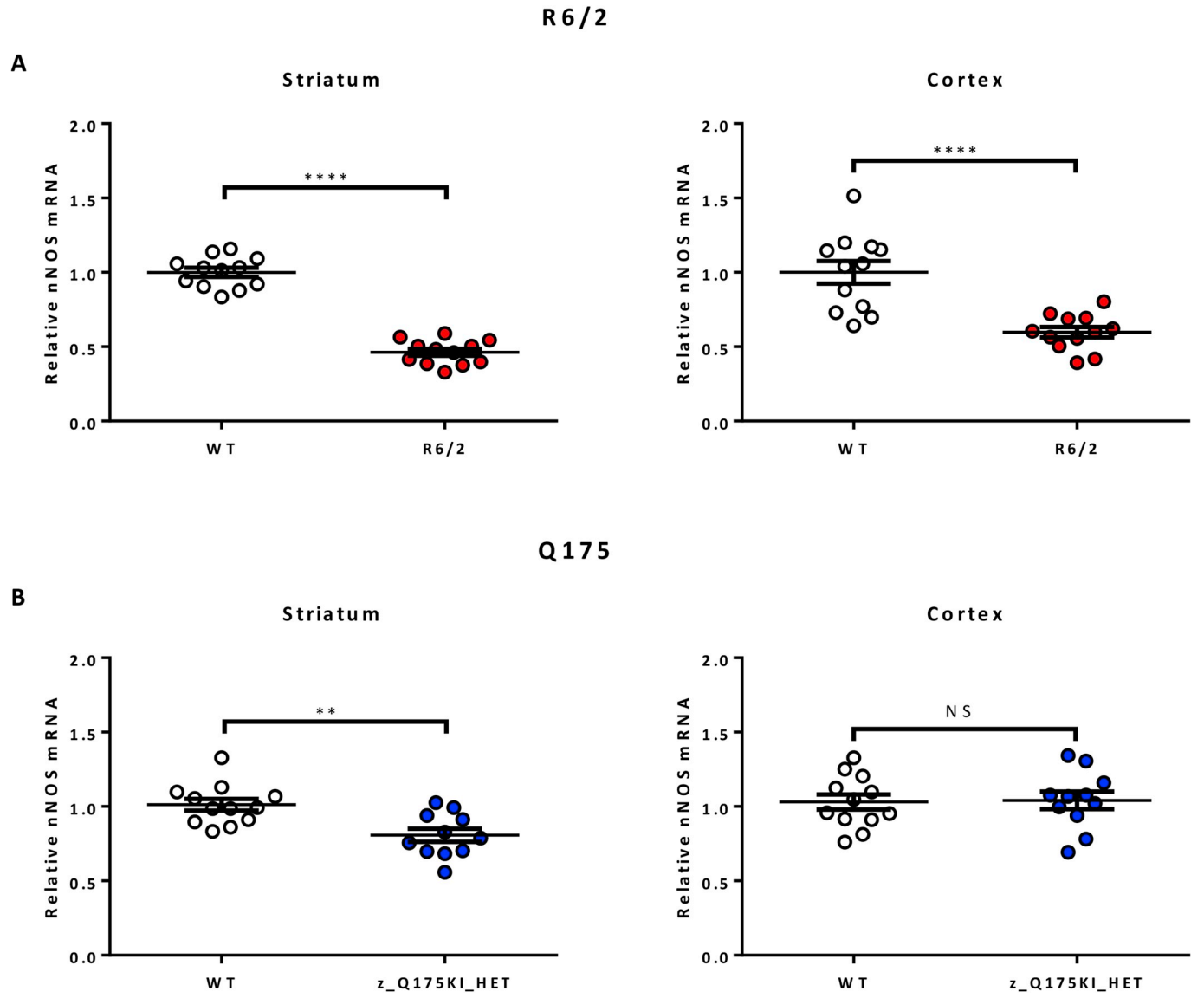

Fig. 5. Between groups comparison of effects of genotype on nNOS transcripts in motor cortex and striatum of WT, R6/2, and Q175 mice. A) nNOS mRNA expression is significantly down-regulated in the striatum (54%) and cortex (40%) of R6/2 mice at 3 months of age (unpaired *t*-test, ****p < 0.0001). Data are derived from 12 WT mice (n = 6 male, n = 6 female) and 14 R6/2 mice (n = 7 male, n = 7 female). **B)** A more modest reduction (19%) of nNOS transcript levels was observed in the striatum of 11.5 month old Q175 mice (unpaired *t*-test, **p < 0.01), whereas the cortex was not affected (p > 0.05; NS, not significant). Data are derived from 12 WT mice (n = 6 male, n = 6 female) and 11 Q175 mice (n = 6 male, n = 5 female).

nitroblue tetrazolium to diformazan, and subsequent histochemical staining of nNOS interneurons [42,43]. Furthermore, we and others have shown that NADPH-d activity in striatal interneurons is sensitive to nNOS inhibitors, NMDA receptor antagonists, dopamine depletion, and D1/2 receptor agonists/antagonists [23,44,45]; [40,46]. We have also found highly complementary results when comparing our studies on the dopaminergic and glutamatergic modulation of striatal nNOS activity performed using NO selective amperometric microsensors [26,47] [25,46,48]; to those using NADPH-d histochemistry [23,40,44,46]. The utility of the histochemical approach is highlighted by our recent study showing that electrical stimulation of the hippocampal fimbria increases both amperometric measures of NO efflux and NADPH-d staining in a nNOS-dependent manner in the medial shell of the nucleus accumbens [46]. Thus, NADPH-d histochemistry can be utilized as an accurate index of nNOS enzyme activity in interneurons in corticostriatal circuits.

In the current study, analyses of all mice (16–21 months old males and females) revealed that Q175 mice exhibited significant overall reductions in NADPH-d staining in the cortex and striatum as compared to WT controls. Examination of the 16 and 21 month old groups separately revealed that the cortex was not affected in Q175 mice until 21 months of age, whereas significant deficits in NADPH-d staining were observed in the striatum at 16 and 21 months of age. qPCR studies also showed that nNOS transcript expression is down-regulated in a striatal-specific manner as early as 11.5 months of age in Q175 mice. These findings are consistent with studies of human postmortem brains from patients with HD which show that NADPH-d staining in the neuropil of the caudate and putamen progressively declines in a manner which correlates with the extent of neurodegeneration [30]. Thus, these authors found that early in the disease the loss of staining is first apparent in the striosomes (grade 0 using the grading scale of Vonsattel [49], whereas in more advanced cases of the disease (grades 1 and 2), an additional loss of staining is observed in the matrix compartment [30]. Consistent with studies showing that nNOS interneurons are spared in the HD striatum [6,8,9], the loss of NADPH-d staining was confined to the neuropil and the number of stained neuronal somata was similar to

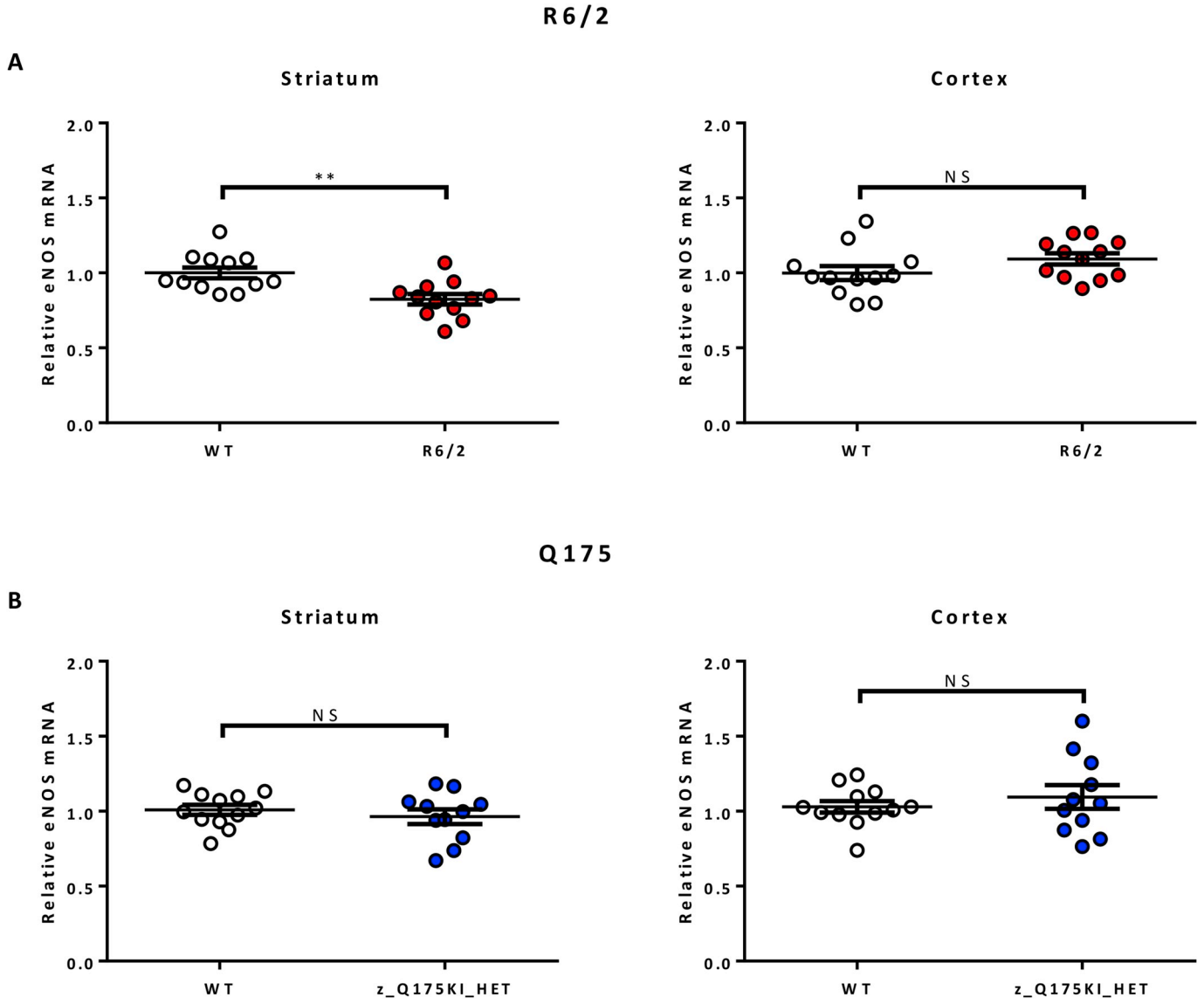

Fig. 6. Between groups comparison of effects of genotype on eNOS transcripts in motor cortex and striatum of WT, R6/2, and Q175 mice. A) eNOS mRNA expression is significantly down-regulated in the striatum (18%, unpaired *t*-test, **$p < 0.01$) but not in the cortex ($p > 0.05$; NS, not significant) of 3 month old R6/2 mice. Data are derived from 12 WT mice (n = 6 male, n = 6 female) and 12 R6/2 mice (n = 6 male, n = 6 female). Cortical and striatal eNOS transcript level is unaffected by knock-in mutant HTT allele in 11.5 month old Q175 mice. Data are derived from 12 WT mice (n = 6 male, n = 6 female) and 11 Q175 mice (n = 6 male, n = 5 female).

controls [30]. Emson and colleagues reported similar progressive losses of nNOS mRNA in the HD striatum which were more profound in late stages (grades 2 and 3) of the disease [19]. Other markers of nNOS interneurons such as somatostatin are also decreased in the CSF [16] and postmortem striatum of HD patients [19]. Changes in nNOS interneurons have not been reported in the sensorimotor cortex in HD patients [19], however this remains to be well studied across early and advanced disease stages.

Consistent with the above human studies and our findings in Q175 mice, R6/1 and R6/2 mouse models of HD exhibit significant decreases in striatal nNOS activity, and nNOS mRNA and protein [10,32–35]. Consistent with our findings of decreased nNOS mRNA expression in R6/2 mice, decreases in nNOS activity and protein have also been reported in the cortex of R6/2 mice [33,34]. In agreement with our qPCR studies in Q175 mice, no significant differences in eNOS activity were found in R6/2 mice compared to controls, indicating that down-regulation of nitrergic transmission in HD may be attributed largely to changes in nNOS interneurons as opposed to endothelial or microglia cells [33,35]. However, we did observe modest but significant decreases in eNOS mRNA expression in the striatum of 3 month old R6/2 mice, suggesting that eNOS activity may become compromised in later stages of the disease.

Interestingly, several of the above studies in HD mouse models have also shown that deficits in striatal nNOS activity are associated with abnormal clasping reflexes and correlated with decreases in body weight and rotarod performance [33–35]. HD transgenic mice treated with nNOS inhibitors also showed accelerated symptom progression that was correlated with the degree of nNOS inhibition measured in activity assays [33]. Moreover, HD mice with a targeted genetic deletion of both copies of the nNOS gene exhibited accelerated disease progression and motor dysfunction compared to heterozygous and WT HD mice [34]. Taken together, the current results and above studies suggest that nNOS activity and NO signaling in corticostriatal circuits are compromised in an age-dependent manner in HD which is associated with disease progression and severity of motor dysfunction (Fig. 7).

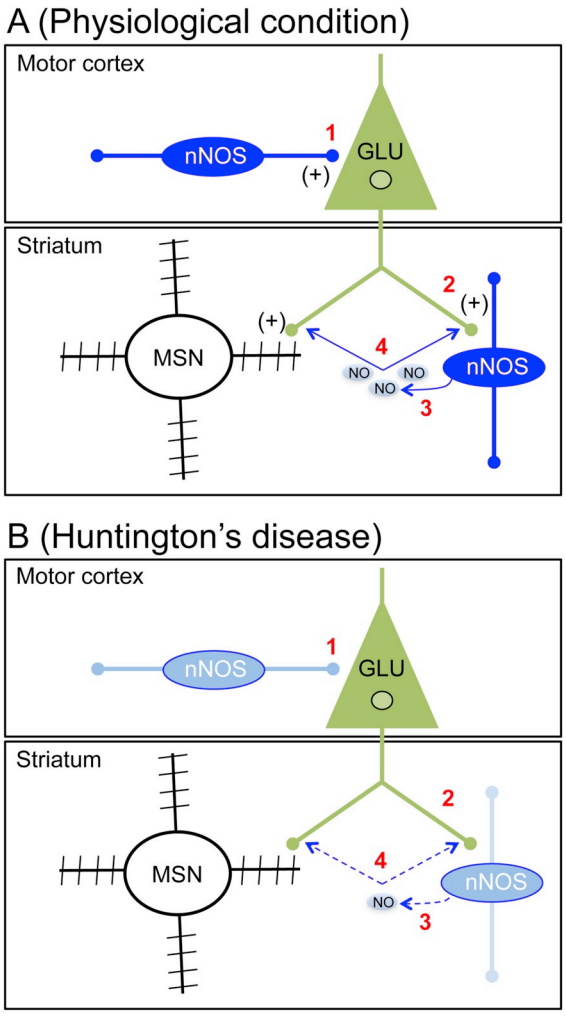

Fig. 7. Schematic illustrating hypothesized role of nNOS in controlling the activity of corticostriatal signaling pathway. A) In normal physiological conditions (1) NO release in cortex would act to facilitate excitability of corticostriatal neurons and their excitatory drive to the striatum. (2) Glutamate released from corticostriatal terminals stimulates NO production (3) in nNOS striatal interneurons. (4) NO released from nNOS striatal interneurons acts to stimulate glutamate release and facilitates corticostriatal transmission. **B)** In HD, nitrergic interneurons are spared but, as demonstrated by qPCR and NADPH-d histochemical measures, nNOS expression and activity is impaired in the striatum of HD mice. Our recent studies in nNOS knockout mice [29] demonstrated that striatal projection neurons were substantially less responsive to cortical drive as compared to WT controls, indicating that tonic NO acts to facilitate corticostriatal transmission in the intact striatum. These observations indicate that decreased nitrergic transmission might contribute to circuit pathophysiology in HD and that pharmacotherapies designed to restore NO signaling may be efficacious treatments for HD.

4.2. Deficits in cortical and striatal nitrergic transmission may contribute to corticostriatal dysfunction in the Q175 mouse model of HD

In later stages of HD (grade 3–4), moderate atrophy of the motor and premotor cortices occur together with striatal MSN loss (reviewed in Vonsattel [49]. Associated degeneration of corticostriatal projection neurons and loss of their striatal connectivity is thought to lead to complex age-dependent dysfunction in glutamatergic corticostriatal transmission and synaptic plasticity [13–15]. Indeed, in vitro and in vivo studies in the Q175 mouse model of HD have demonstrated that functional deficits in glutamatergic corticostriatal transmission arise between 6 and 9 months of age, a time period when heterozygous animals exhibit an overt HD behavioral phenotype [21,36,38,50]. Additionally, morphological abnormalities including reductions in cortical and striatal volume, occur at 8 months of age in Q175 mice [50]. Moreover, significant decreases in spine density of MSNs were present at 7 and 12 months of age [36]. Corticostriatal projection neurons recorded in Q175 mice also exhibited increased sIPSC frequencies and IPSC to EPSC ratios at 12 months of age compared with age-matched WT controls [36]. Taken together, the above studies indicate that by 12 months of age (full HD behavioral phenotype), significant neuroanatomical and neurophysiological deficits exist in cortical and striatal circuits of Q175 mice.

In addition to depolarizing the membrane potential and driving spike activity in striatal MSNs, cortical stimulation also depolarizes and evokes action potentials in striatal nNOS interneurons identified using NADPH-d histochemistry and immunocytochemistry for nNOS [51,52]. Moreover, the high (30 Hz), but not low ($\leq$3 Hz) frequency firing of synchronized corticostriatal neuronal networks may preferentially drive spike activity and NO synthesis in striatal nNOS interneurons via glutamatergic activation of NMDA receptors [24–26,53]. Furthermore, pharmacological [24,26,48,54,55] and genetic [29] disruption of NO signaling has been shown to strongly depress the responsiveness of striatal MSNs to corticostriatal transmission (reviewed in Refs. [27,28]. Given the above, the observed decrease in cortical and striatal NADPH-d activity in aged Q175 mice would be expected to result in compromised nitrergic signaling and deficits in NO-dependent facilitation of corticostriatal transmission (Fig. 7).

4.3. Sex-dependent deficits in neuronal NOS activity in the Q175 mouse model of HD

While evidence exists for sex differences in age of onset and disease duration/severity in patients with HD [56,57] and animal models [58–61], a clear picture of the impact of gender on the pathophysiology of HD has not emerged. However, the majority of the above studies in HD models suggest that male HD mice exhibit more prominent neuropathology and motor deficits potentially due to neuroprotective effects of estrogen in females. The current results showing that female Q175 mice exhibited modest decreases in NADPH-d staining which were not statistically significant are consistent with the above studies. Stronger correlations between cortical and striatal NADPH-d staining intensity were also observed in males in both age groups. These observations point to age-dependent deficits in nNOS activity in corticostriatal circuits of Q175 mice which are more pronounced in males.

5. Conclusions

Observations from the current studies demonstrate that deficits in NADPH-d staining, a measure of nNOS activation, and nNOS transcript expression are present in the motor cortex and striatum in late stages of experimental HD and progress in a more severe manner in male Q175 mice. Based on previous studies, this age-dependent loss of nitrergic transmission would be expected to contribute to deficits in corticostriatal glutamatergic transmission [29] and exacerbate circuit and motor dysfunction observed in HD models [13–15]. Given that these age-dependent decreases in NO synthesis are more robust in relatively old male mice (21 months of age), it is likely that male HD patients in the later stages of the disease might benefit from pharmacotherapies designed to augment nitrergic signaling and corticostriatal transmission (e.g., sodium nitroprusside; cyclic nucleotide phosphodiesterase (PDE) inhibitors).

Acknowledgements

This work was supported by the Chicago Medical School and CHDI Foundation, Inc.

Appendix A. Supplementary data

Supplementary data to this article can be found online at https://doi.org/10.1016/j.niox.2018.12.002.

References

[1] The Huntington's Disease Collaborative Research Group, A novel gene containing a trinucleotide repeat that is expanded and unstable on Huntington's disease chromosomes. The Huntington's Disease Collaborative Research Group, Cell 72 (1993) 971–983.

[2] R.L. Albin, A. Reiner, K.D. Anderson, J.B. Penney, A.B. Young, Striatal and nigral neuron subpopulations in rigid Huntington's disease: implications for the functional anatomy of chorea and rigidity-akinesia, Ann. Neurol. 27 (4) (1990) 357–365.

[3] M. DiFiglia, E. Sapp, K.O. Chase, S.W. Davies, G.P. Bates, J.P. Vonsattel, N. Aronin, Aggregation of huntingtin in neuronal intranuclear inclusions and dystrophic neurites in brain, Science 277 (5334) (1997) 1990–1993.

[4] A. Reiner, R.L. Albin, K.D. Anderson, C.J. D'Amato, J.B. Penney, A.B. Young, Differential loss of striatal projection neurons in Huntington disease, Proc. Natl. Acad. Sci. Unit. States Am. 85 (15) (1988) 5733–5737.

[5] A. Reiner, E. Shelby, H. Wang, Z. DeMarch, Y. Deng, N.H. Guley, V. Hogg, R. Roxburgh, L.J. Tippett, H.J. Waldvogel, R.L. Faull, Striatal parvalbuminergic neurons are lost in Huntington's disease: implications for dystonia, Mov. Disord. 28 (12) (2013) 1691–1699.

[6] L.M. Canzoniero, A. Granzotto, D.M. Turetsky, D.W. Choi, L.L. Dugan, S.L. Sensi, nNOS (+) striatal neurons, a subpopulation spared in Huntington's Disease, possess functional NMDA receptors but fail to generate mitochondrial ROS in response to an excitotoxic challenge, Front. Physiol. 4 (2013).

[7] F. Cicchetti, L. Prensa, Y. Wu, A. Parent, Chemical anatomy of striatal interneurons in normal individuals and in patients with Huntington's disease, Brain Res. Rev. 34 (1) (2000) 80–101.

[8] D. Dawbarn, M.E. De Quidt, P.C. Emson, Survival of basal ganglia neuropeptide Y-somatostatin neurones in Huntington's disease, Brain Res. 340 (2) (1985) 251–260.

[9] R.J. Ferrante, N.W. Kowall, M.F. Beal, E.P. Richardson Jr., E.D. Bird, J.B. Martin, Selective sparing of a class of striatal neurons in Huntington's disease, Science 1985 (4725) (1985) 561–563.

[10] B. Zucker, R. Luthi-Carter, J.A. Kama, A.W. Dunah, E.A. Stern, J.H. Fox, D.G. Standaert, A.B. Young, S.J. Augood, Transcriptional dysregulation in striatal projection- and interneurons in a mouse model of Huntington's disease: neuronal selectivity and potential neuroprotective role of HAP1, Hum. Mol. Genet. 14 (2) (2005) 179–189.

[11] E.H. Aylward, N.B. Anderson, F.W. Bylsma, M.V. Wagster, P.E. Barta, M. Sherr, J. Feeney, A. Davis, A. Rosenblatt, G.D. Pearlson, C.A. Ross, Frontal lobe volume in patients with Huntington's disease, Neurol. 50 (1) (1998) 252–258.

[12] H.D. Rosas, W.J. Koroshetz, Y.I. Chen, C. Skeuse, M. Vangel, M.E. Cudkowicz, K. Caplan, K. Marek, L.J. Seidman, N. Makris, B.G. Jenkins, Evidence for more widespread cerebral pathology in early HD an MRI-based morphometric analysis, Neurol. 60 (10) (2003) 1615–1620.

[13] K.D. Bunner, G.V. Rebec, Corticostriatal dysfunction in Huntington's disease: the basics, Front. Hum. Neurosci. 10 (2016).

[14] M.D. Sepers, L.A. Raymond, Mechanisms of synaptic dysfunction and excitotoxicity in Huntington's disease, Drug Discov. Today 19 (7) (2014) 990–996.

[15] C. Cepeda, N. Wu, V.M. André, D.M. Cummings, M.S. Levine, The corticostriatal pathway in Huntington's disease, Prog. Neurobiol. 81 (5) (2007) 253–271.

[16] H. Cramer, J. Kohler, G. Oepen, G. Schomburg, E. Schröter, Huntington's chorea—measurements of somatostatin, substance P and cyclic nucleotides in the cerebrospinal fluid, J. Neurol. 225 (3) (1981) 183–187.

[17] S. Gines, I.S. Seong, E. Fossale, E. Ivanova, F. Trettel, et al., Specific progressive cAMP reduction implicates energy deficit in presymptomatic Huntington's disease knock-in mice, Hum. Mol. Genet. 12 (2003) 497–508.

[18] A.L.O. Hebb, H.A. Robertson, E.M. Denovan-Wright, Striatal phosphodiesterase mRNA and protein levels are reduced in Huntington' s disease transgenic mice prior to the onset of motor symptoms, Neuroscience 123 (4) (2004) 967–981.

[19] P.J. Norris, H.J. Waldvogel, R.L. Faull, D.R. Love, P.C. Emson, Decreased neuronal nitric oxide synthase messenger RNA and somatostatin messenger RNA in the striatum of Huntington's disease, Neuroscience 72 (4) (1996) 1037–1047.

[20] S.U. McKinstry, Y.B. Karadeniz, A.K. Worthington, V.Y. Hayrapetyan, M.I. Ozlu, K. Serafin-Molina, W.C. Risher, T. Ustunkaya, I. Dragatsis, S. Zeitlin, H.H. Yin, Huntingtin is required for normal excitatory synapse development in cortical and striatal circuits, J. Neurosci. 34 (28) (2014) 9455–9472.

[21] V. Beaumont, et al., Phosphodiesterase 10A inhibition improves cortico-basal ganglia function in Huntington's disease models, Neuron 92 (6) (2016) 1220–1237.

[22] D. Zwilling, S.Y. Huang, K.V. Sathyasaikumar, F.M. Notarangelo, P. Guidetti, H.Q. Wu, J. Lee, J. Truong, Y. Andrews-Zwilling, E.W. Hsieh, J.Y. Louie, Kynurenine 3-monooxygenase inhibition in blood ameliorates neurodegeneration, Cell 145 (6) (2011) 863–874.

[23] K.E. Hoque, R.P. Indorkar, S. Sammut, A.R. West, Impact of dopamine-glutamate interactions on striatal neuronal nitric oxide synthase activity, Psychopharmacol. 207 (4) (2010) 571–581.

[24] J.M. Ondracek, A. Dec, K.E. Hoque, S.A. Lim, G. Rasouli, R.P. Indorkar, J. Linardakis, B. Klika, S.J. Mukherji, M. Burnazi, S. Threlfell, S. Sammut, A.R. West, Feed-forward excitation of striatal neuron activity by frontal cortical activation of nitric oxide signaling in vivo, Eur. J. Neurosci. 27 (2008) 1739–1754.

[25] D.J. Park, A.R. West, Regulation of striatal nitric oxide synthesis by local dopamine and glutamate interactions, J. Neurochem. 111 (2009) 1457–1465.

[26] S. Sammut, D.J. Park, A.R. West, Frontal cortical afferents facilitate striatal nitric oxide transmission in vivo via a NMDA receptor and neuronal NOS-dependent mechanism, J. Neurochem. 103 (3) (2007) 1145–1156.

[27] A.R. West, K.Y. Tseng, Nitric oxide–soluble guanylyl cyclase–cyclic GMP signaling in the striatum: new targets for the treatment of Parkinson's disease? Front. Syst. Neurosci. 5 (2011).

[28] A.R. West, Nitric oxide signaling in the striatum, in: H. Steiner, K.Y. Tseng (Eds.), Handbook of Basal Ganglia Structure and Function, a Decade of Progress, second ed., Elsevier Inc. Academic Press, London, UK, 2016.

[29] F.E. Padovan-Neto, S. Sammut, S. Chakroborty, A.M. Dec, S. Threlfell, P.W. Campbell, V. Mudrakola, J.F. Harms, C.J. Schmidt, A.R. West, Facilitation of corticostriatal transmission following pharmacological inhibition of striatal phosphodiesterase 10A: role of nitric oxide-soluble guanylyl cyclase-cGMP signaling pathways, J. Neurosci. 35 (14) (2015) 5781–5791.

[30] A.J. Morton, L.F.B. Nicholson, R.L.M. Faull, Compartmental loss of NADPH diaphorase in the neuropil of the human striatum in Huntington's disease, Neuroscience 53 (1) (1993) 159–168.

[31] A.W. Deckel, Nitric oxide and nitric oxide synthase in Huntington's disease, J. Neurosci. Res. 64 (2001) 99–107.

[32] S. Cipriani, E. Bizzoco, M. Gianfriddo, A. Melani, M.G. Vannucchi, F. Pedata, Adenosine A 2A receptor antagonism increases nNOS-immunoreactive neurons in the striatum of Huntington transgenic mice, Exp. Neurol. 213 (1) (2008) 163–170.

[33] A.W. Deckel, A. Gordinier, D. Nuttal, V. Tang, C. Kuwada, R. Freitas, K.A. Gary, Reduced activity and protein expression of NOS in R6/2 HD transgenic mice: effects of L-NAME on symptom progression, Brain Res. 919 (1) (2001) 70–81.

[34] A.W. Deckel, V. Tang, D. Nuttal, K. Gary, R. Elder, Altered neuronal nitric oxide synthase expression contributes to disease progression in Huntington's disease transgenic mice, Brain Res. 939 (1) (2002) 76–86.

[35] F. Perez-Severiano, B. Escalante, P. Vergara, C. Ríos, J. Segovia, Age-dependent changes in nitric oxide synthase activity and protein expression in striata of mice transgenic for the Huntington's disease mutation, Brain Res. 951 (1) (2002) 36–42.

[36] T. Indersmitten, C.H. Tran, C. Cepeda, M.S. Levine, Altered excitatory and inhibitory inputs to striatal medium-sized spiny neurons and cortical pyramidal neurons in the Q175 mouse model of Huntington's disease, J. Neurophysiol. (Bethesda) 113 (7) (2015) 2953–2966.

[37] L. Menalled, D. Brunner, Animal models of Huntington's disease for translation to the clinic: best practices, Mov. Disord. 29 (11) (2014) 1375–1390.

[38] L.B. Menalled, A.E. Kudwa, S. Miller, J. Fitzpatrick, J. Watson-Johnson, N. Keating, M. Ruiz, R. Mushlin, W. Alosio, K. McConnell, D. Connor, Comprehensive behavioral and molecular characterization of a new knock-in mouse model of Huntington's disease: zQ175, PloS One 7 (12) (2012) e49838.

[39] G. Paxinos, K.B.J. Franklin, The Mouse Brain in Stereotaxic Coordinates, fourth ed., Academic Press, London, 2012.

[40] K.E. Hoque, A.R. West, Dopaminergic modulation of nitric oxide synthase activity in subregions of the rat nucleus accumbens, Synapse 66 (2012) 220–231.

[41] S.E. Lazic, Statistical evaluation of methods for quantifying gene expression by autoradiography in histological sections, BMC Neurosci. 10 (2009) 5.

[42] T.M. Dawson, D.S. Bredt, M. Fotuhi, P.M. Hwang, S.H. Snyder, Nitric oxide synthase and neuronal NADPH diaphorase are identical in brain and peripheral tissues, Proc. Natl. Acad. Sci. U.S.A. 88 (1991) 7797–7801.

[43] B.T. Hope, G.J. Michael, K.M. Knigge, S.R. Vincent, Neuronal NADPH diaphorase is a nitric oxide synthase, Proc. Natl. Acad. Sci. U.S.A. 88 (1991) 2811–2814.

[44] B.J. Morris, C.S. Simpson, S. Mundell, K. Maceachern, H.M. Johnston, A.M. Nolan, Dynamic changes in NADPH-diaphorase staining reflect activity of nitric oxide synthase: evidence for a dopaminergic regulation of striatal nitric oxide release, Neuropharmacology 36 (1997) 1589–1599.

[45] G. Sancesario, M. Giorgi, V. D'Angelo, A. Modica, A. Martorana, M. Morello, C.P. Bengtson, G. Bernardi, Down-regulation of nitrergic transmission in the rat striatum after chronic nigrostriatal deafferentation, Eur. J. Neurosci. 20 (2004) 989–1000.

[46] K.E. Hoque, S.R. Blume, S. Sammut, A.R. West, Electrical stimulation of the hippocampal fimbria facilitates neuronal nitric oxide synthase activity in the medial shell of the rat nucleus accumbens: modulation by dopamine D1 and D2 receptor activation, Neuropharmacology (2017), https://doi.org/10.1016/j.neuropharm.2017.09.005.

[47] S. Sammut, A. Dec, D. Mitchell, J. Linardakis, M. Ortiguela, A.R. West, Phasic dopaminergic transmission increases NO efflux in the rat dorsal striatum via a neuronal NOS and a dopamine D(1/5) receptor-dependent mechanism, Neuropsychopharmacology 31 (2006) 493–505.

[48] S. Sammut, K.E. Bray, A.R. West, Dopamine D(2) receptor-dependent modulation of striatal NO synthase activity, Psychopharmacol. 191 (3) (2007) 793-80.

[49] J.P.G. Vonsattel, Huntington disease models and human neuropathology: similarities and differences, Acta Neuropathol. 115 (1) (2008) 55–69.

[50] T. Heikkinen, K. Lehtimäki, N. Vartiainen, J. Puoliväli, S.J. Hendricks, J.R. Glaser, A. Bradaia, K. Wadel, C. Touller, O. Kontkanen, J.M. Yrjänheikki, Characterization of neurophysiological and behavioral changes, MRI brain volumetry and 1H MRS in zQ175 knock-in mouse model of Huntington's disease, PloS One 7 (12) (2012) e50717.

[51] Y. Kawaguchi, Neostriatal cell subtypes and their functional roles, Neurosci. Res. 27 (1997) 1–8.

[52] A. Sharott, N.M. Doig, N. Mallet, P.J. Magill, Relationships between the firing of identified striatal interneurons and spontaneous and driven cortical activities in vivo, J. Neurosci. 32 (2012) 13221–13236.

[53] P. O'Donnell, A.A. Grace, Cortical afferents modulate striatal gap junction permeability via nitric oxide, Neuroscience 76 (1997) 1–5.

[54] S. Sammut, S. Threlfell, A.R. West, Nitric oxide-soluble guanylyl cyclase signaling regulates corticostriatal transmission and short-term synaptic plasticity of striatal projection neurons recorded in vivo, Neuropharmacology 58 (2010) 624–631.
[55] A.R. West, A.A. Grace, The nitric oxide-guanylyl cyclase signaling pathway modulates membrane activity states and electrophysiological properties of striatal medium spiny neurons recorded in vivo, J. Neurosci. 24 (2004) 1924–1935.
[56] J.K. Lee, Y. Ding, A.L. Conrad, E. Cattaneo, E. Epping, K. Mathews, J.S. Perlmutter, Sex-specific effects of the Huntington gene on normal neurodevelopment, J. Neurosci. Res. 95 (1–2) (2017) 398–408.
[57] R.A. Roos, M. Vegter-Van Der Vlis, J. Hermans, H.M. Elshove, A.C. Moll, J.J. Van de Kamp, G.W. Bruyn, Age at onset in Huntington's disease: effect of line of inheritance and patient's sex, J. Med. Genet. 28 (8) (1991) 515–519.
[58] F.J. Bode, M. Stephan, H. Suhling, R. Pabst, R.H. Straub, K.A. Raber, C. Sjoberg, Sex differences in a transgenic rat model of Huntington's disease: decreased 17β-estradiol levels correlate with reduced numbers of DARPP32+ neurons in males, Hum. Mol. Genet. 17 (17) (2008) 2595–2609.
[59] B. Connor, Y. Sun, D. Von Hieber, S.K. Tang, K.S. Jones, C. Maucksch, AAV1/2-mediated BDNF gene therapy in a transgenic rat model of Huntington's disease, Gene Ther. 23 (3) (2016) 283.
[60] J.L. Dorner, B.R. Miller, S.J. Barton, T.J. Brock, G.V. Rebec, Sex differences in behavior and striatal ascorbate release in the 140 CAG knock-in mouse model of Huntington's disease, Behav. Brain Res. 178 (1) (2007) 90–97.
[61] D.A. Kuljis, L. Gad, D.H. Loh, Z.M. Kaswan, O.N. Hitchcock, C.A. Ghiani, C.S. Colwell, Sex differences in circadian dysfunction in the BACHD mouse model of Huntington's disease, PloS One 11 (2) (2016) e0147583.